

See discussions, stats, and author profiles for this publication at: <https://www.researchgate.net/publication/268487639>

# Design and experimental verification of an intelligent wall-climbing welding robot system

**Conference Paper** in *Industrial Robot the international journal of robotics research and application* · September 2014

DOI: 10.1142/9789814623353\_0014

---

CITATIONS

6

---

READS

273

8 authors, including:



**Yonglong Li**

Sichuan Energy Internet Research Institute, Tsinghua University

25 PUBLICATIONS 304 CITATIONS

SEE PROFILE

# Design and experimental verification of an intelligent wall-climbing welding robot system

Zhongcheng Gui, Yongjun Deng, Zhongxi Sheng, Tangjie Xiao, Yonglong Li, Fan Zhang,  
Na Dong and Jiandong Wu

Intelligent Equipment & Control Technology Institute, Dongfang Electric Corporation R&D Center, Chengdu, China

## Abstract

**Purpose** – This paper aims to present a new intelligent wall-climbing welding robot system for large-scale steel structure manufacture, which is composed of robot body, control system and welding system.

**Design/methodology/approach** – The authors design the robot system according to application requirements, validate the design through simulation and experiments and use the robot in actual production.

**Findings** – Experimental results show that the robot system satisfies the demands of automatic welding of large-scale ferromagnetic structure, which contributes much to on-site manufacturing of such structures.

**Practical implications** – The robot can work with better quality and efficiency compared with manual welding and other semi-automatic welding devices, which can much improve large-scale steel structure manufacturing.

**Originality/value** – The robot system is a novel solution for large-scale steel structures welding. There are three major advantages: the robot body with reliable adsorption ability, large payload capability and good mobility which meet the requirements of welding; the control system with good welding seam tracking accuracy and intelligent automatic welding ability; and friendly human – computer interface which makes the robot easy to use.

**Keywords** Mobile robots, Robot welding

**Paper type** Research paper

## 1. Introduction

With the rapid development of computer science and manufacture technology, industrial welding robots have been widely used in the structured environment, such as the automotive industry and the electronic industry. However, there is still no effective solution of welding robots serving in large-scale steel structure manufacture industry such as ship assembly and large container production. In general, those large-scale steel structures are unique. Furthermore, they are so huge and heavy that they are mostly welded on-site. The traditional industrial welding robots become inapplicable in these situations. At present, this kind of structure is mainly manually welded, and this method features heavy labor intensity, poor working environment, unreliable welding quality and low welding productivity. So the automatic welding solution for large-scale steel structure manufacture is urgently needed.

This paper presents a novel, intelligent, wall-climbing welding robot system (IWWRS) for large-scale steel structure manufacture. The remainder of this paper proceeds in the following order. After a brief introduction of related work, an

overview of IWWRS is presented, followed by a detailed description of the mechanical design and the control system. A set of experimental results are then presented to demonstrate and verify the properties of IWWRS, followed by concluding remarks on the validation of the overall system.

## 2. Related work

A number of researchers are investigating new solutions based on mobile welding robot, and several approaches have been proposed. One approach uses fixed-track to determine the welding direction and provide fixation (Cao *et al.*, 2009; Kim *et al.*, 2008; Shen *et al.*, 2005). Those fixed-track welding robots with pre-installation of tracks are partly efficient for straight seams on plane surfaces. Although some flexible tracks can make robots to adapt to curved surfaces with a smooth radius, the high installation requirements and the impossibility of mounting tracks into narrow spaces make their application limited. Another approach is based on a mobile platform with multi degrees, which provides the possibility of fully automatic tracking and welding. MRWS (Stracy and Canfield, 2012) uses two continuous permanent magnet tracks to provide the freedom of mobile platform and the adsorption force, but the welding process is remotely controlled by man. NOMAD (Mulligan and Melton, 2005) uses a robot transport vehicle to carry a six-axis

The current issue and full text archive of this journal is available at  
[www.emeraldinsight.com/0143-991X.htm](http://www.emeraldinsight.com/0143-991X.htm)



Industrial Robot: An International Journal  
41/6 (2014) 500–507  
© Emerald Group Publishing Limited [ISSN 0143-991X]  
[DOI 10.1108/IR-08-2014-0384]

This paper is an extended and updated version of the paper presented at the 17th International Conference on Climbing and Walking Robots (CLAWAR), Poznan, Poland, 21–23 July 2014, where it received the Industrial Robot Journal ‘Highly Commended’ award for practical innovation.

robot; at the same time, a global vision system is used for location and orientation, which results in automatic welding. A wheeled welding robot (Wu et al., 2011) with a structure magnet can lift the wheel and change adhesion force using one motor so that the robot has the ability to passing obstacles, which expands the range of application. Zhang et al. (2003) introduces a wheeled autonomous mobile welding robot system which has four wheels to act as a car driving. The sensing system for seam tracking is based on a rotating arc sensor, so the robot can weld automatically.

While those researches have resulted in a large number of conceptual welding robots, there is still no product brought into commercial practice. Many improvements (Gui, 2007) are still in need: the reliability of adsorption, the flexibility of movement, the intelligence of welding and the accuracy of tracking.

### 3. IWWRS overview

IWWRS consists of robot body, control system and welding system. The robot can climb ferromagnetic structures in any orientation, and the newly designed adsorption device and moving mechanism allow for climbing on curved surface. The seam tracking algorithm and control system make the welding process intelligent; as a result, IWWRS can weld automatically with little manual intervention to adapt to the actual variational conditions. The dimensions of the robot body are 820 mm × 885 mm × 734 mm, the weight is approximately 60 kg and the payload capacity can be up to 60 kg, which meets the requirement of carrying a welding gun, sensor package and other cables. The robot body includes the mobile platform and manipulator; the control system comprises the main control system, field control box and sensing system; the welding system includes the welding power supply units, wire feeder, protective gas and welding cooling system (Figure 1).

### 4. Mechanical design of the robot body

The robot body of IWWRS shall have three basic functions:

- 1 movement is all-positioned and flexible enough to climb the flat or curved surface of the workpiece;
- 2 adsorption force can meet the payload to carry welding tools such as a welding gun; and
- 3 freedom of manipulator can satisfy the need of posture and position adjustment of the welding gun.

Figure 1 Composition of robot system



Based on the modular design method, the robot body includes two parts: mobile platform and manipulator, as shown in Figure 2.

#### 4.1. Mobile platform

Several forms of instability may happen when the robot stay in the stationary state. According to the three-wheeled structure, as shown in Figure 3, considering the gravity (G) and the friction, the minimum total equivalent adsorption force applied on the two rear driving wheels is:

To prevent slip:

$$F_{\text{slip}} = \frac{\sqrt{((\mu_s - \mu_r)H + L)^2 + (\mu_r S + \mu_s (L - S))^2}}{\mu_s L} G - \frac{\mu_r}{\mu_s} F_{ms} \quad (1)$$

To prevent longitudinal overturning:

$$F_{\text{LongO}} = \frac{\sqrt{H^2 + S^2}}{L} G \quad (2)$$

Figure 2 Robot body is composed of manipulator and mobile platform

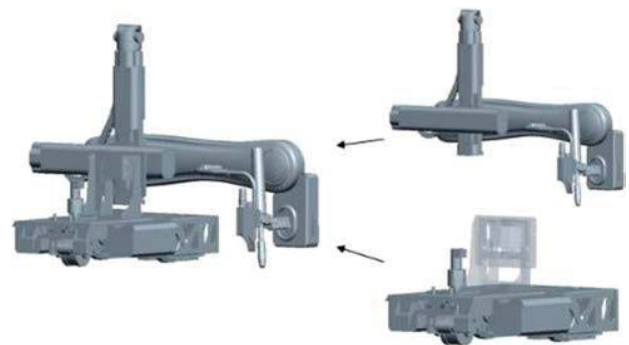
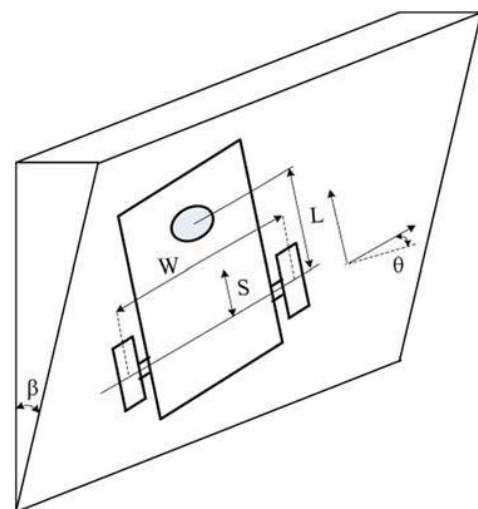


Figure 3 Mechanical analysis model of the mobile platform. W, S, L are the dimension parameters, and  $\theta$ ,  $\beta$  are the posture parameters



To prevent transverse overturning:

$$F_{TransverseO} = -F_{ms} + \frac{\sqrt{4H^2 + W^2}}{W}G \quad (3)$$

To prevent lateral overturning:

$$F_{LateralO} = \sqrt{\left(\frac{2H}{W\sin(\arctan(2L/W))}\right)^2 + \left(\frac{(L-S)}{L}\right)^2}G \quad (4)$$

Where  $\mu_s$  is sliding friction coefficient,  $\mu_r$  is rolling friction coefficient,  $H$  is the distance between surface and the center of gravity,  $S$  is the distance between the axis of two rear driving wheels and the center of gravity,  $G$  is the gravity of the robot and  $F_{ms}$  is the adsorption force of front supporting wheel. In the motion state, adsorption force must be strong enough to prevent the driving wheel from slipping. The minimum total equivalent adsorption force applied on the two rear driving wheels  $F_{mD}$  can be deduced as:

$$F_{mD} = \frac{2\mu_r F_{mS} L}{W(\mu_s - \mu_r)} + \left[ \left( \left( \frac{1}{(\mu_s - \mu_r)} + \frac{2\mu_r H}{W(\mu_s - \mu_r)} + \frac{H}{L} \right) c_\theta \right) c_\beta + \left( \frac{2S}{W(\mu_s - \mu_r)} - \frac{2H}{W} \right) s_\theta + \left( \frac{-2\mu_r S}{W(\mu_s - \mu_r)} + \frac{(L-S)}{L} \right) s_\beta \right] G \quad (5)$$

Where  $s^* = \sin(^*)$ ,  $c^* = \cos(^*)$ . According to equations (1–5), under the same condition, the larger the parameters of  $W$ ,  $L$  and  $\mu_s$  are, the more stable the system will be. This rule is used to determine the dimension parameters; moreover, the minimum adsorption force needed can be computed accordingly.

Adsorption device is the core of the mobile platform; IWWRs adopts a new adsorption structure which comprises arrayed gapped adsorption and magnetic wheel adsorption. Permanent magnet arrays are installed in the bottom of the mobile platform, where is close to the driving wheels. Several millimeters gap, which can be adjusted, exists between the arrays and the workpiece. The supporting wheel, which is directly in contact with the walking surface, is installed with a permanent magnet. The adsorption force is mainly provided by permanent magnet arrays.

A three-wheeled structure is applied on this mobile platform, which can ensure the robot to adapt to curved surfaces and get small turning radius. All the wheels are driven separately. The supporting wheel is set as the front wheel, which is used for orientation. Another two wheels are set as rear wheels, which are used to provide driving force, and the mobile platform is differentially driven. The mobile platform can realize the movement of turning in place.

#### 4.2. Manipulator

Manipulator performs the actual actions of the welding gun, which include movements in X/Y direction and expected swing motions. So, manipulator comprises a crosshead slipper and a swing device.

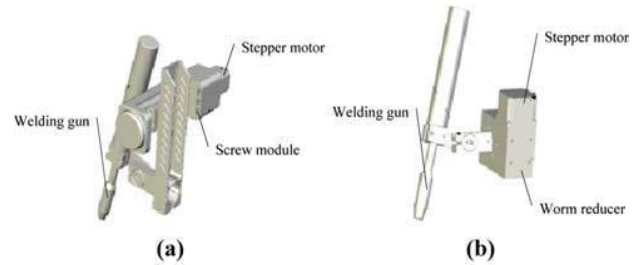
Crosshead slipper uses a commercial precision product; the key technical indicators are determined by workspace, control precision and payload. To improve efficiency and the weld forming, the local swing motion is expected. Parallel swing and angle swing are the common swing types, as shown in Figure 4. On the parallel swing device, stepper motor and screw module are connected through the coupling; the welding gun moves along the screw axis with the motor driving force. On the angle swing device, stepper motor is directly connected to worm reducer, whose transmission ratio is 60.

With the crosshead slipper and the swing device, the manipulator has three degrees of freedom: horizontal movement, vertical movement and swing.

#### 4.3. Simulation

According to the mechanical design of the robot body, system-level simulation with ADAMS is taken to verify the performance of IWWRs, as shown in Figure 5. The simulation results show that, both on the plane and curved surfaces, IWWRs moves smoothly and stably in all postures and in all position.

Figure 4 CAD model of two different swing devices



Notes: (a) Parallel swing device; (b) angle swing device

Figure 5 System-level simulation. Different moving orientations and posture conditions are simulated according to the demand of all-position movement



## 5. Control system

The control system of IWWRS is developed with taking into account actual working condition. Control system includes five parts:

- 1 electrical system;
- 2 sensing system;
- 3 motion control system;
- 4 communication system; and
- 5 human – machine interaction system.

Some detail functions are outlined in Table I. Most of the control algorithm is executed on a programmable computer controller (PCC).

### 5.1. Hardware composition for control system

According to the function and layout division, hardware of control system is divided into four parts:

- 1 on-body hardware;
- 2 off-body hardware;
- 3 robot-control pendant; and
- 4 welding device interface.

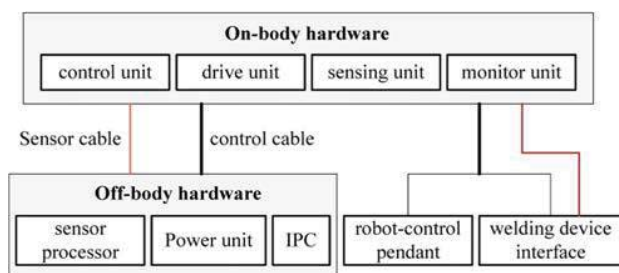
The layout is shown in Figure 6.

On-body hardware is installed on the robot body. Control unit applies PCC X20 system produced by B&R to process signals and realize advanced language programming. Drive unit includes stepper motor drive, brush DC motor drive and brushless DC motor drive. Drive unit is designed to be distributed and realizes the integration with PCC through

Table I Control system framework

Control subsystem	Detail function
Electrical system	Electrical wiring Electric source Safety interlock
Sensing system	Laser vision sensing Photoelectric displacement sensing; gyroscope sensing
Motion control system	Mobile platform control Crosshead slipper control Swing device control Seam track control
Communication system	Communication with welding device Bus communication of PCC
Human – machine interaction system	Robot-control pendant Remote operating software

Figure 6 The layout diagram of control hardware



CANOpen bus. Sensing unit is composed of laser vision sensor, photoelectric displacement sensor and gyroscope sensor. Laser vision sensor can recognize seam position; photoelectric displacement sensor can obtain robot position with the three wheels' encoder value; gyroscope sensor can return the reliable posture information. Monitor unit uses a vision sensor to observe the welding pool during welding.

Off-body hardware is placed in an industrial-designed control cabinet. Sensor processor is used to process laser vision information and transmit the effective data to PCC through RS232. Power unit includes three switching power supplies: 12V, 24V and 48V. IPC includes host computer, dust-tight keyboard and industry display monitor. Operator can monitor working state of robot and perform remote control through IPC.

Robot-control pendant is a hand-held device, used to perform field control and human intervene. The central processing module is designed based on ARM Cortex-M3 framework; the operating instruction input module includes buttons and knobs; TFT LCD is used to display the state and parameters of controlled objects. The central processing module receives and processes control instructions, sending control signals to PCC through CAN bus.

Welding device communicates with PCC through a special interface card which uses DeviceNet protocol.

### 5.2. Software solution for control system

On the system architecture, IWWRS is divided into three layers: the HMI layer, communication layer and the lower-level software layer, as shown in Figure 7.

The HMI, responsible for welding vision monitoring, mobile platform control and crosshead slipper control, is composed of IPC and robot-control pendant. Through HMI the operators can configure the parameters, send instructions and monitor the robot status. The HMI of IPC includes four parts:

- 1 welding monitor main page;
- 2 motion monitor page;
- 3 welding preparation page; and
- 4 system configuration page, as shown in Figure 8.

The communication layer is implemented with multiple types of protocols, including industrial Ethernet (between the IPC and the PCC), RS232/RS485 (between the PCC and the laser vision sensor), DeviceNet (between the PCC and the welding device), CANOpen (between the PCC and the step motors), digital I/O, etc.

Figure 7 Software architecture of IWWRS

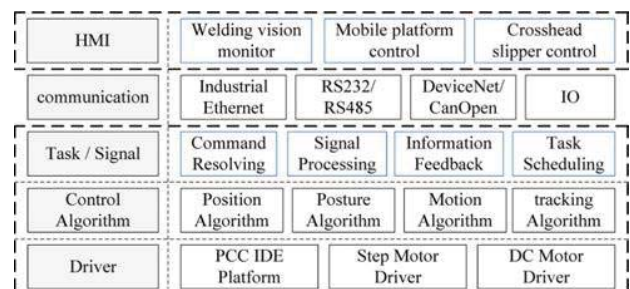
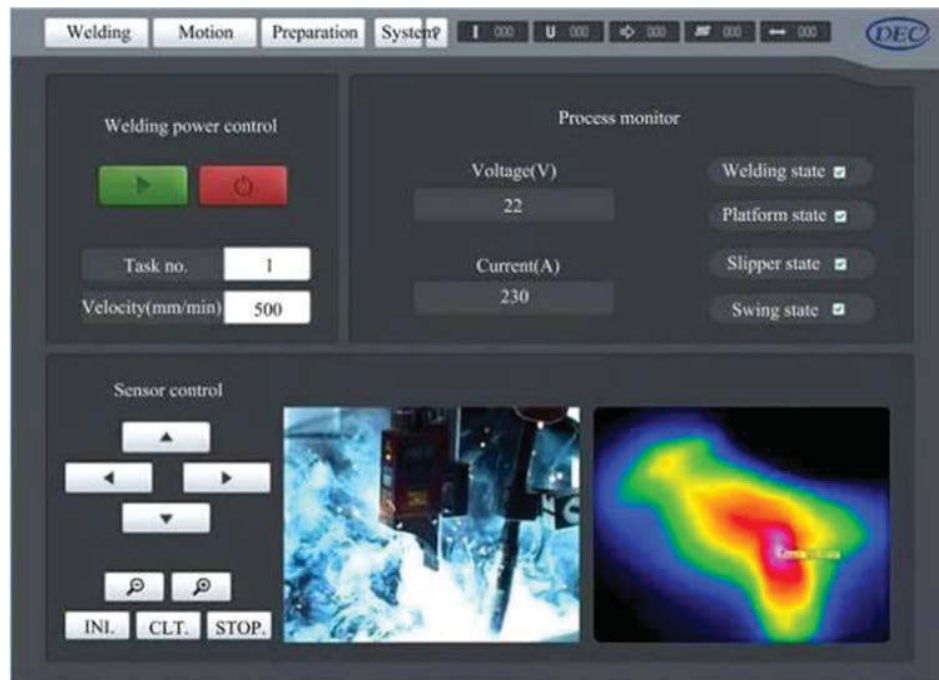




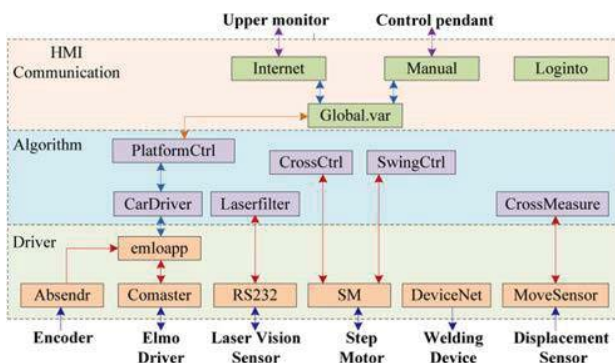
Figure 8 The HMI of IWWRS, running on the under-body host computer



The lower-level software layer is the most critical layer in this architecture. It integrates the code for command resolving, signal processing, information feedback and task scheduling; implements the control algorithms for determination of position and posture, motion control and seam tracking; and also contains the driver for step & DC motors.

The software of PCC achieves the task of HMI, communication, device driver and control algorithm. The device driver function includes motor driver, welding device driver and so on. The control algorithm includes the crosshead slipper control, platform control and swing control. The B&R X20 PCC has the feature of multitasking, which is used to divide the software of PCC into different modules. Each module change the data through the global variable. So it realizes the cooperation development of the software. Relation of the different modules is shown in Figure 9.

Figure 9 Relation of the different modules of PCC



### 5.3. Control algorithm

Control algorithm of IWWRS, aimed at keeping the welding gun moving on the correct path with a constant speed, mainly includes two parts: platform control and crosshead slipper control. By applying PID algorithm, crosshead slipper control realizes the position closed loop control, while platform control realizes the double closed loop control of position and posture.

#### 5.3.1 Sensor data filtering algorithm

Laser vision sensing data which are the main input signal of the control algorithm are vulnerable to arc interference. The data sent back from the laser vision sensor may largely deviate from the true value. If corresponding measures are not taken, these error data will result in the unexpected response of crosshead slipper. To eliminate the noise and outliers, a sensor data filtering algorithm combining time-series data stream prediction technique and error threshold elimination is researched. According to the data just before the current time point and the motion principles of the robot, the algorithm estimates the data of the current time and makes judgment on the sensor data based on the preset threshold values. If the detection result is wrong, the data of the previous moment will be adopted for control, and the data of the current moment will be added to the prediction of next moment. The prediction expression is described as in equation (6):

$$P_{est} = \frac{\sum_{n=1}^{10} P_n \times k_n}{\sum_{n=1}^{10} k_n} \quad (6)$$

Where  $P_{est}$  is estimate value,  $P_n$  is data of the  $n$  period and  $k_n$  is weighted value. Comparing the estimate value and the real data, if the difference is above the threshold value, this value is considered to be faulty.

### 5.3.2 Posture estimated algorithm

Because of the mechanical structure, there is a distance between laser vision sensor and the end of manipulator. Control algorithm is focused on the end of manipulator, sensor data can't reflect the real position of the expected control point, so the compensation algorithm for sensor data is based on the angle between seam direction and moving direction the mobile platform is involved in. The module of robot motion is shown in Figure 10.

When angle  $\alpha$  is estimated, the mobile platform move distance is  $S$ , and  $D$  is computed from the data of laser vision sensor data and crosshead slipper movement. The least square estimate method is used to compute the angle  $\alpha$ ; the expression is described as in equation (7):

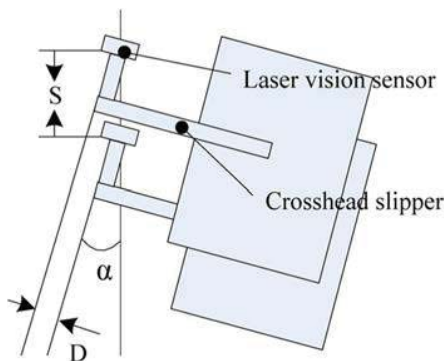
$$\theta = \arcsin \left[ \frac{n \sum_{i=1}^n S_i D_i - \sum_{i=1}^n S_i \sum_{i=1}^n D_i}{n \sum_{i=1}^n S_i^2 - \left( \sum_{i=1}^n S_i \right)^2} \right] \quad (7)$$

Where  $n$  is the number of recorded points,  $S_i$  and  $D_i$  are separately the real-time values of  $S$  and  $D$ . Those angles are unable to compensate the advanced error because they are non-continuous. To solve this problem, gyroscope sensing data and Kalman (Sasiadek and Khe, 2001) are used, the expression is shown below:

$$\begin{cases} \bar{x}_k = A\bar{x}_{k-1} + B u_{k-1} \\ \bar{p}_k = A\bar{p}_{k-1} A^T + Q \\ k_k = \bar{p}_k H^T (H\bar{p}_k H^T + R)^{-1} \\ x_k = \bar{x}_k + k_k (z_k - H\bar{x}_k) \\ p_k = (I - k_k H) \bar{p}_k \end{cases} \quad (8)$$

According to the model of platform, the parameters can be determined based on experimental results, where  $u$  is the angle calculated by encoder value and gyroscope sensing data;  $z$  is the angle calculated with the least squares method. Then the

**Figure 10** The module of robot motion.  $D$  is the adjusted distance,  $S$  is the moved distance,  $\alpha$  is the angle between the robot and the seam to track



accurate angle value can be calculated and used to estimate the posture of the mobile platform.

### 5.3.3 Crosshead slipper control algorithm

Step motor of the crosshead slipper is the aimed control object. Position sensor installed on the shaft of step motor feeds back position offset which is taken as input signal, and output signal is the motor drive signal. The principle of crosshead slipper control is shown in Figure 11.

PI controller has fast response without steady-state error. We use engineering stabilizing method to primarily determine the PI control parameters, and obtain the final parameters with good dynamic characteristics through a set of experiments.

### 5.3.4 Mobile platform control algorithm

The structure of mobile platform uses a three-wheeled type: differentially driven by two rear wheels with a motor singly, guided by a front wheel with two motors. The mobile platform control is equivalent to the control with the four motors. Through the analysis of moving, geometrical expressions such as equations (9), (10) and (11) can be deduced:

$$\theta = \arctan \left( \frac{v_c}{-\omega_c H} \right) \quad (9)$$

$$\begin{bmatrix} v_L \\ v_R \end{bmatrix} = \begin{bmatrix} 1/d & -L/2d \\ 1/d & L/2d \end{bmatrix} \begin{bmatrix} v_c \\ \omega_c \end{bmatrix} \quad (10)$$

$$v_F = \sqrt{v_c^2 + (\omega_c \times H)^2} \quad (11)$$

Where  $v_c$  is the expected forward velocity;  $\omega_c$  is the expected angular velocity of rotation. The target angular velocity  $\theta$  of the front wheel can be calculated based on  $v_c$  and  $\omega_c$ .  $d$  is the wheel radius and  $L$  is the distance between the two rear wheels.  $v_L$   $v_R$   $v_F$  are separately the velocities of left driving wheel, right driving wheel and front wheel, respectively. Through equations (10) and (11), the three velocities can be obtained.

Mobile platform control algorithm makes the robot adjust position and posture in wide range. Two control loops including position closed loop and posture closed loop are designed based on PID algorithm. The principle of mobile platform control is shown in Figure 12.

**Figure 11** The principle of crosshead slipper control

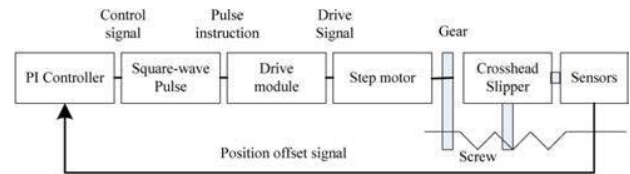
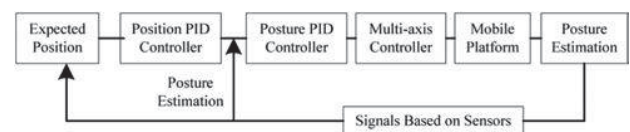


**Figure 12** The principle of mobile platform control



## 6. Experimental verification

This section presents a set of experiments to verify IWWRS's performance in a factory of large-scale power equipment manufacturing. First, the test for climbing performance is carried out; then, different seam conditions are applied to verify the tracking property; finally, procedure qualification experiment and product welding examples are launched to verify the welding properties, including the quality and efficiency.

### 6.1. Climbing performance verification

In the factory, we choose several typical products with plane and curved surfaces for IWWRS to climb on. For the curved surface, the radii of curvature include 3.25 m and 1.89 m. IWWRS climbs in all directions, including vertical direction and horizontal direction, and the maximum velocity can reach 2 m/min, which is enough for welding. During the climbing tests, the mobile platform can absorb reliably on the plane and curved surfaces and move flexibly. The payload can reach up to 60 kg, which is enough to carry the welding gun, sensors and other conventional tools. The vertical and horizontal climbing test is shown in Figure 13.

### 6.2. Tracking property verification

The tracking property is realized by the coordinated control of mobile platform and manipulator. Mobile platform tracking is mainly affected by the angle between the seam and forward direction in the initial state, while manipulator control is mainly based on the laser vision sensing data, which are affected by actual seam conditions such as gap change and groove offset. When the velocity is set as 200 mm/min, a series of initial angles is set, and the time of turning mobile platform to the direction along the tracked seam is recorded. The result is outlined in Table II.

The time of angle adjustment is acceptable for welding; at the same time, the welding gun always points to the seam during turning and the speed forward is stable. So the operating demand for initial installation of mobile platform is not strict, and this advantage can signally improve the adaptability of IWWRS.

**Figure 13** The photos of IWWRS climbing on the cylindrical products



**Table II** The time test of angle adjustment

Angle (degree)	–30	–15	15	30
Time (s)	48	30	28	52

**Note:** The direction of the tracked seam is fixed in advance. The initial angles between the fixed seam and mobile platform are measured with a precise angle measurement instrument according to the central axis of IWWRS

The special workpieces with grooves of X and V type are used to verify the manipulator tracking property. Although the gap changes from 2 mm to 5 mm and the maximum groove offset is 6 mm, IWWRS can track the seam stably.

Several tracking experiments are carried out to verify the accuracy of tracking. The initial goal center of groove is set to –16.5 mm in the sensor coordinate, and the tracked center of groove is detected in real time by laser vision sensor. The velocity is set as 200 mm/min, and the tracking length is 2 m. One typical result is shown in Figure 14. The data prove that the accuracy of the tracking is below 1 mm.

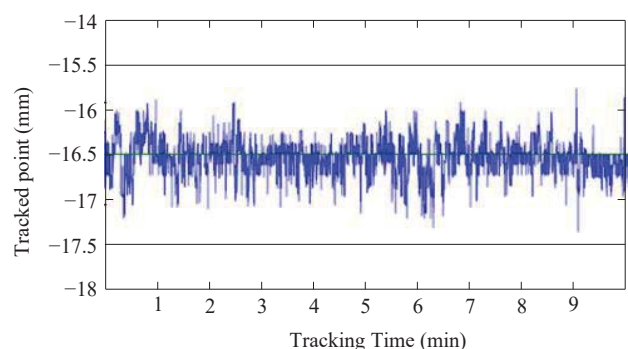
### 6.3. Welding verification

The welding system is established with a Fronius Electric Power TPS5000 welding machine, a VR1500 wire feeder and a Binzel ROBO650 automatic welding gun. Welding method is GMAW. Welding wires include metal powder-cored wire and solid wire, and protective gas is rich-argon mixing gas.

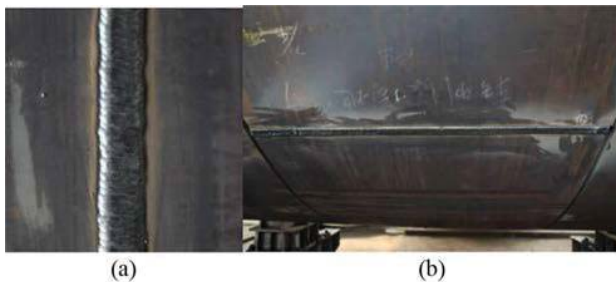
The procedure qualification experiment is the first step of welding verification. The material of standard sample is Q235 low-carbon steel, which is common in large-scale structure manufacture. The V type groove has a 45-degree angle and a root opening of 2 mm. IWWRS finishes the welding with five beads: 110 A, 16.5 V, 90 mm/min for the bottom bead; 200 A, 21 V, 100 mm/min for the three filling beads; 220 A, 22 V, 75 mm/min for the covering head. The weld has no visual cracks, undercuts or voids, and the ultrasonic inspection result shows that the weld has no voids or incomplete fusion. The procedure qualification experimental result shows that the GMAW performed by IWWRS can meet the requirement for low carbon steel welding.

To verify the running properties of IWWRS, five pieces of actual products are selected to weld. Two low-pressure shells of turbine used in thermal power station construction are applied to verify horizontal welding, while three cylindrical end shields of gas turbine power unit are applied to verify vertical welding. Horizontal welding applies solid wire and vertical welding applies powder-cored wire. IWWRS finishes the welding of the key seams with a higher efficiency and a higher quality compared with manual welding. Not only are there no visual defects such as undercuts, but also there are no internal defects such as incomplete fusion. The consistency of weld quality is fine. Figure 15 shows a vertical welding sample. For a horizontal seam with 35 mm thickness and 5 m length, IWWRS welding costs about 3 hours, while manual welding

**Figure 14** Typical tracking data of IWWRS





**Figure 15** Products welded by IWWRS

**Notes:** Local view (a) and global view; (b) show the welding result

need at least 4 hours. All the five products are examined to satisfy the quality requirements of power equipment, and have come into use in power station construction.

## 7. Conclusion

IWWRS is a novel solution for large-scale structures welding. There are several advantages: reliable adsorption ability; huge payload capability which meets the requirements of welding and good mobility; intelligent control system which can satisfy the demands of welding and tracking accuracy; and friendly human – computer interface. IWWRS can weld intelligently so that the non-value-added preparing time for the traditional automatic welding systems can be eliminated.

The mechanical design of the robot body is based on sufficient theoretical calculations. The compound adsorption structure which comprises both arrayed gapped adsorption and magnetic wheel adsorption provides enough payload and flexible moving performance. Manipulator with crosshead slipper and swing device perform the expected local welding motions.

The intelligent control hardware and software systems are designed based on PCC. The hardware system includes electrical system, sensing system, motion control system, communication system and human – computer interaction system, while the software system includes the HMI layer, communication layer and the lower-level software layer. The tracking algorithm is the core of control algorithm. IWWRS tracks the seam with a coordinated control algorithm based on sensor fusion. During the tracking, the mobile platform control algorithm is executed to track in a wide range, while the crosshead slipper control algorithm is executed to track on the local level.

Several cylindrical products are used to test climbing performance, and the results verify that IWWRS can move flexibly on the curved surface with velocity up to 2 m/min. Several tracking experiments are carried out to verify the accuracy of tracking, and the results show that IWWRS can perform tracking without strict tapering operation, the angle adjusting time is short and the tracking accuracy is below 1 mm. Finally, the welding system is established. The results of the procedure qualification experiment and the products

welding process show that IWWRS is stable and reliable, and the efficiency and quality are much improved compared with manual welding.

IWWRS has been applied in welding of large-scale power equipments in our factory at scale, and series engineering products development will be performed to meet different kinds of products' welding requirements in the near future.

## Note

1. This paper is an extended and updated version of the paper presented at the 17th International Conference on Climbing and Walking Robots (CLAWAR), Poznan, Poland, 21–23 July 2014, where it received the *Industrial Robot Journal* “Highly Commended” award for practical innovation.

## References

- Cao, Y., Xue, L. and Cui, W. (2009), “Research on flexible rail type spherical tank welding robot”, *Electric Welding Machine*, Vol. 39 No. 4, pp. 68–70.
- Gui, Z.C. (2007), “Study on wall climbing robot for hydraulic turbine blade on-site repair”, *PhD dissertation*, Department of Mechanical Engineering, Tsinghua University, Beijing.
- Kim, J., Lee, K.Y. and Kim, T., Lee, D., Lee, S., Lim, C. and Kang, S.W. (2008), “Rail Running Mobile Welding Robot ‘RRX3’ for Double Hull Ship Structure”, *Proceedings of 17th World Conference of International Federation of Automatic Control*, Seoul.
- Mulligan, S. and Melton, G. (2005), “Autonomous welding of large steel fabrications”, *Industrial Robot: An International Journal*, Vol. 32 No. 4, pp. 346–349.
- Sasiadek, J.Z. and Khe, J. (2001), “Sensor fusion based on fuzzy Kalman filter”, *Proceedings of the 2nd International Workshop on Robot Motion and Control*, Bukowy Dworek.
- Shen, W., Gu, J. and Shen, Y. (2005), “Proposed wall climbing robot with permanent magnetic tracks for inspecting oil tanks”, paper presented at IEEE International Conference of Mechatronics and Automation, Niagara Falls, Ont.
- Stracy, J. and Canfield, S. (2012), “Theoretical and empirical verification of a mobile robotic welding platform”, *Welding Journal*, Vol. 91, pp. 338–345.
- Wu, M., Gao, X. and Yan, W., Fu, Z., Zhao, Y. and Chen, S. (2011), “New mechanism to pass obstacles for magnetic climbing robots with high payload, using only one motor for force-changing and wheel-lifting”, *Industrial Robot: An International Journal*, Vol. 38 No. 4, pp. 372–380.
- Zhang, H., Wang, H., Xu, J.N. and Lou, S.N. (2003), “A new wheeled autonomous mobile welding robot system based on rotating arc sensor”, *Robot*, Vol. 25 No. 6, pp. 536–538.

## Corresponding author

**Zhongcheng Gui** is the corresponding author and can be contacted at: [guizc@dongfang.com](mailto:guizc@dongfang.com)